A Simple Means for Reducing the Risk of Progressive Collapse

Yihai Bao, H.S.Lew, Fahim Sadek, and Joseph Main

Biography:

Yihai Bao is an IPA researcher in the Engineering Laboratory at the National Institute of Standards and Technology (NIST). He received his BS and MS degrees from Tongji University of China and PhD from the University of California, Davis. His research interests include nonlinear modeling of structural behavior under extreme loading conditions, large-scale experimental methods and advanced scientific computational methods.

H. S. Lew, Honorary Member ACI, is a senior research engineer in the Engineering Laboratory (EL) at the National Institute of Standards and Technology (NIST). He received his PhD from the University of Texas at Austin, and is a licensed professional engineer. He has served on the ACI Board of Direction and the Technical Activities Committee. He is a member of ACI Committee 318, Concrete Research Council, and other ACI committees. His research interests include performance of structural members and systems, construction safety, failure investigations and earthquake engineering.

Fahim Sadek is Leader of the Structures Group in the Engineering Laboratory (EL) at the National Institute of Standards and Technology (NIST). He received his PhD from the Southern Methodist University, and is a licensed professional engineer. His research interests include vulnerability of structures subjected to multi-hazard conditions, response of structures to dynamic and impulse loading and structural health monitoring.

Joseph Main is a research structural engineer in the Engineering Laboratory (EL) at the National Institute of Standards and Technology (NIST). He received his PhD from Johns Hopkins

University. His research interests relate to the computational assessment of structural performance under extreme loads, including wind loading, air-blast loading, and loading generated by abnormal events such as fire, explosions and vehicular impacts.

ABSTRACT

A simple debonding technique is proposed to reduce or eliminate strain localization in reinforcing bars in the region of wide flexural cracks in RC beams to enhance the resistance of RC buildings to disproportionate collapse (also refer to as progressive collapse). Debonding was achieved by heat shrinking polyolefin tube over the reinforcing bar. The experimental results show that testing of a #8 reinforcing bar imbedded in concrete with 8-in (203 mm) debonding on both sides of a ¼ in (6.35 mm) wide gap (simulating a flexural crack) allowed the bar to stretch before fracture about 38 percent more than the bar without debonding. This shows clearly that the debonding method can effectively reduce strain localization, thereby delaying the fracture of reinforcing bar. To analyze the debonding behavior, detailed finite- element models of the test specimens were developed. Good agreement between the computational and experimental results validated the computational method used in this study. Intermediate moment frame (IMF) beam-column assemblies were analyzed by applying the validated debonding model under a column removal scenario. The results show improvements of more than 30 percent in the vertical load carrying capacity with a debonding length of twice the depth of beam. This indicates that debonding enhances the development of catenary action in beams of RC frame structures.

Keywords: buildings; caternary action; computational model; concrete structures; debonding; disproportionate collapse; testing.

Disclaimer: Certain trade names or company products are mentioned in the text to specify adequately certain products. In no case does identification imply recommendation or endorsement by the National Institute of Standards and Technology, nor does it imply the product is the best available for the purpose.

BACKGROUND

Recent tests of planar subassemblies of a ten-story reinforced concrete frame structure, comprising two beams and three columns, have shown that the development of catenary action in the beams under a center column loss scenario is limited by fracture of flexural tension reinforcement (Lew et al. 2013). Similar behavior has been observed in other tests of RC frames or assemblies under column removal scenarios (Yi et al. 2008, Su et al. 2009, and Yu and Tan 2011). Most of the tested specimens failed in a similar manner, which was due to reinforcing bar fracture in tension at the beam ends. Figure 1 shows one of the bottom reinforcing bars fractured at a wide flexural crack developed at the beam-center column interface during the sub-frame assembly test. Strain localization occurred in the exposed bar segment at the crack, due to the greater axial constraint provided by concrete bonded to the embedded bar segments on each side of the crack. Computational models based on a validated, detailed finite element analysis of the intermediate moment frame (IMF) assembly (Bao et al. 2012) confirmed the existence of this strain localization, which is evident as a sharp increase of strain in the beam bottom reinforcing

bars near the unsupported center column (see results with no debonding in Fig. 2). Debonding the reinforcing bar from the surrounding concrete could reduce the strain localization (see results with debonding length = $1.0D$ in Fig. 2, where D is the beam depth) and thereby delay the fracture of reinforcing bars. This enables the beam to sustain larger rotations and increase catenary forces prior to fracture, and to increase the vertical load-carrying capacity under a column removal scenario.

Figure 3 illustrates the concept of using a debonding technique to release the strain localization at dominant crack openings. In practice, de-bonded zones are located at the beam ends. In Fig. 2, evenly-distributed strain along the bar segment near the center column is seen when reinforcing bars are allowed to slide freely along the longitudinal direction with a debonding length equal to one depth of the beam section. Details about modeling bond stress between reinforcing bars and concrete are provided by Bao et al. (2012).

Based on the aforementioned concept, a simple approach is proposed herein to achieve debonding between reinforcing bars and the surrounding concrete. This approach is also validated through an experimental study. Furthermore, its effectiveness in resisting disproportionate collapse (commonly known as progressive collapse) is verified by computational analysis. The optimum debonding length and the behavior under seismic loading conditions are also evaluated numerically.

EXPERIMENTAL INVESTIGATION

Three specimens were investigated under uniaxial tensile load to demonstrate (1) the effectiveness of a technique used in this study to debond reinforcing bars from the surrounding concrete and (2) the efficacy of debonding reinforcing bars at a cracked zone in delaying the fracture of bars and providing enhanced ductile behavior.

Specimen Design

Each specimen consists of two 10 in × 48 in (254 mm × 1219 mm) concrete cylinders which are connected by one No. 8 reinforcing bar (Fig. 4). The quarter-inch (6.4 mm) gap between the two cylinders represents a crack opening. The specimen is to be pulled in the longitudinal direction until reinforcing bar fracture occurs. The force is applied through the T-shaped steel loading fixture at each end of the specimen. The force was transmitted to the specimen by means of four high-strength 7/8 in (22.2 mm) diameter threaded bars which were connected to the 2 in (51 mm) thick circular steel disk which served as the flange of the T section of the loading fixture. A round-shaped high-strength paper tube was used as the formwork. Debonding the reinforcing bars from surrounding concrete was achieved by using polyolefin shrink tube covering the desired location of reinforcing bars. Under heat treatment, the tube shrinks in the radial direction to fit tightly over the bar. Fig. 5 shows a tube section on a reinforcing bar before and after subjecting to a heat source. Three specimens (A, B, and C) were built with different debonding lengths on each side of the gap: no debonding, 2 in (51 mm) debonding, and 8 in (203 mm) debonding, respectively.

Material Properties

The specimens were designed with self-consolidating concrete having a nominal compressive strength of 6 ksi (41.4 MPa) and ASTM A706-Grade 60 reinforcing bars with a minimum specified yield strength of 60 ksi (414 MPa). An average compressive strength of concrete from testing of three 6 in × 12 in (152 mm × 305 mm) cylinders at the time of testing was 12 ksi (83 MPa). The measured yield and ultimate strengths of the No. 8 bars were 70 ksi (483 MPa)

and 103 ksi (710 MPa), respectively. The yield strain was 0.265 % and the fracture strain was 16 % with a gage length of 8 in (203 mm).

Instrumentation and Test Setup

Strain gages were placed on the bar surface over a length of 8 in (203 mm) on each side of the gap to measure the strain along the center reinforcing bar. The relative movement between two cross-sections located at 3 in (76 mm) away from the gap was measured by displacement transducers. Tensile loading was applied under displacement control at a rate of 0.15 in/min (3.8 mm/min). A schematic of the test setup is shown in Fig. 4 along with the photograph of the test machine and specimen.

Experimental Results

The specimens were loaded continuously until failure occurred. For all three specimens, failure was characterized by the fracture of the central reinforcing bar within the 1/4 in (6.4 mm) gap. Figure 6 shows a cone-shaped concrete failure emanating from the central reinforcing bar to the free surface which was formed for the specimen without debonding (Specimen A). However, no significant concrete damage to the free surface was observed for the specimens with debonding (Specimen B and C). The confinement provided by the surrounding concrete at the end of the debonding zone resisted concrete damage for Specimens B and C, while concrete spalled at the free surface for Specimen A, (See Figures 6a and 6b). Fig. 7a shows a plot of the applied load versus displacement for the three specimens based on experimental and computational results. The displacement was measured using two displacement transducers over a 6.25 in (159 mm) gage length (Fig. 4). While the peak load is almost identical for the three specimens, significant

differences are observed among the peak displacements of the three specimens prior to failure. The specimen without debonding (Specimen A) failed at a displacement of about 1.45 in (37 mm), while Specimen B, with a debonding length of 2 in (51 mm), failed at a smaller displacement of approximately 0.9 in (23 mm), and Specimen C, with a debonding length of 8 in (203 mm), failed at a larger displacement of approximately 2 in (51 mm).

These results show that debonding over a very short length can actually result in earlier fracture than having no debonding. The reason is that de facto debonding (loss of bond) occurs under loading for the specimen without debonding, within a cone-shaped region of extensive concrete damage. If the debonding length is less than the extent of this damage zone for a fully bonded specimen, then strains in the reinforcing bar are localized within a shorter length of the debonded zone, resulting in earlier fracture. This explains why Specimen A shows more ductile behavior than Specimen B, which has a short debonding length of 2 in (51 mm). However, debonding length of 8 in (203 mm), which was applied to Specimen C, increases the peak displacement by about 38 perceent when compared with the fully bonded Specimen A. This clearly indicates that the debonding method, when applied over a sufficient length, can effectively delay the fracture of the reinforcing bar.

COMPUTATIONAL ANALYSIS

Analysis of Axially Loaded Cylindrical Prism test

Detailed finite element models of the three test specimens were developed in this study using the LS-DYNA (Hallquist 2007) general purpose software package. Concrete was modeled using 8-node solid elements with mesh size about 1 in (25 mm), while reinforcing bars were represented by 2-node beam elements (Fig. 7b) with mesh size of 2 in (51 mm). Mesh sensitivity study was performed that a further refined mesh doesn't give the inconsistent results. A continuous surface

cap model was used as the material model for concrete. The main features of the model including: isotropic constitutive equations, a yield surface formulated in terms of three stress-invariant shear surface with translation for pre-peak hardening, a hardening cap that expands and contracts, damage-based softening with erosion and modulus reduction, and rate effects for high strain rate applications. Bond behavior between concrete elements and reinforcing bars was simulated by adding one-dimensional contact which only allows movement along the longitudinal direction based on predefined bond-slip relationship, and prevents penetration normal to the bar axis (Hallquist 2007). Debonding between reinforcing bars and surrounding concrete was achieved by setting a very small value of the bond modulus (Ratio of bond stress to slip). Due to the space limitation, further modeling details can be found in the reference paper by Bao et al. (2012). Plots of the applied load versus displacement for the three specimens tested are shown in Fig. 7a along with the experimental results. Good agreement between computational and experimental results validates the computational method used in this study. As observed experimentally, the computational results show that the shorter debonding length of 2 in (51 mm) actually reduces the deformation capacity relative to the fully bonded specimen, while the longer debonding length of 8 in (203 mm) increases the deformation capacity. Selected results from the analysis of Specimen C are presented in Fig. 7b. The damage contours indicate some level of concrete damage starting at about 8 in (203 mm) from the gap, corresponding to the location where the concrete was fully bonded to the central reinforcing bar. The axial force shown along the central reinforcing bar is fairly constant within the debonded zone and gradually decreases further along the length due to bond effects in the fully bonded zone.

Debonding length

The debonding length in a reinforced concrete beam starting from the face of the column may be expressed as $n \times D$, where n is a numerical factor and D is the depth of beam. A parametric study was carried out to determine the optimum value of the factor n that would produce the best performance for an IMF beam-column assembly which was tested and analyzed under a column removal scenario prior to bar fracture and beam failure. The design of the testing specimens was in accordance with ACI Building Code Requirements for Structural Concrete (ACI 318-02) and Commentary (ACI 318R-02). Detail information on the test program was presented in the paper by Lew et al. (2013). The IMF assembly was analyzed with debonding length of 0 (no debonding), $1D$, $2D$ and $3D$, respectively, to determine the optimum debonding length which results in the largest displacement and peak load prior to bar fracture and beam failure, without adversely affecting the stiffness of the beam. The computational model was validated with the experimental data for the case of no debonding (Bao et al. 2012). Figure 8 depicts the applied vertical load versus the vertical displacement of the center column, based on analyses with different n values. The figure shows that the debonding length of $3D$ provided the best performance (largest vertical load and displacement prior to failure). Since the differences in peak loads prior to failure between the cases with $2D$ and $3D$ were not significant, it is prudent to use $2D$ as the optimum length of debonding to avoid adversely impacting the stiffness of the connection by using a larger debonding length. The results show improvements of more than 30% in the peak load with a debonding length of 2D for the IMF beam-column assembly analyzed herein.

SEISMIC PERFORMANCE

Both the experimental and computational investigations showed that the proposed debonding method can effectively eliminate strain localization of reinforcing bars at wide cracks.

Computational models showed that debonding of reinforcing bars at the beam ends in a beam-column assembly significantly increases the catenary resistance under a column loss scenario. However, a potential concern with application of the proposed debonding method is whether it might result in degraded performance under seismic loading.

To examine the effect of debonding the bottom reinforcement next to the column face under seismic loading conditions, a finite element model of a cruciform beam-column assembly was developed and subjected to lateral loading at the top of the cruciform. The cross sectional dimensions and reinforcement details of the cruciform are same as the IMF assembly (Lew et al. 2013). The lengths of the upper and lower columns are both 6 ft (1829 mm), and the lengths of the beams are 10 ft (3048 mm). The same modeling technique that was used before for the IMF assembly was employed for this model. Two loading conditions were considered as shown in Fig. 9: (1) monotonic, pushover displacement and (2) cyclic displacement. For each loading case, analyses were conducted (1) without debonding (DL = 0 in Fig. 9) and (2) with a debonding length of DL = 2.0D. The applied load versus the lateral displacement response at the top of the column for the monotonic and cyclic load is shown in Figs. 9a and 9b, respectively. In both loading cases, a small degradation in stiffness was seen in the responses from the cruciform with DL = 2.0 D. However, the overall response indicates that debonding the bottom reinforcing bars in the vicinity of the beam-column interface would have only a minor effect on the seismic resistance of the structure. It should point out that the bar buckling was not modeled in the current model. Additional study is required to investigate whether the proposed debonding technique could affect the bucking behavior.

The debonding method presented herein is assumed to be applied to a continuous reinforcing bar. When a lap splice or bar cutoff occurs at the reinforcing bar that is to be debonded, adequate

anchorage must be assured to develop the tensile strength of the reinforcing bar. Only the bottom reinforcing bars are proposed to be debonded to avoid undesirable impacts on the connection stiffness. In general, the negative bending moment capacity of beam end sections is larger than the positive bending moment capacity. Therefore, the bottom reinforcing bars are likely to fracture before the top reinforcing bars under a column loss scenario.

CONCLUSIONS

Recent experimental results for reinforced concrete beam-column assemblies under a column removal scenario indicate that prior to failure of the assembly, tensile catenary forces develop in the beam as the beam-column joint deflection exceeds the beam depth, supplying additional gravity load-carrying capacity. However, this load-resisting mechanism is limited by the rotational capacity at the beam ends. Experimental observations indicate that the failure of the assembly is characterized by fracture of the bottom reinforcing bars at a major crack opening near the beam-column interface. Results of detailed finite element models of the beam-column assembly indicate that strain localization within the crack opening causes an early fracture of reinforcement, which limits the beam-end rotational capacity. The method proposed is based on the idea that such strain localization can be mitigated or eliminated if the reinforcing bar is debonded from the surrounding concrete in zones where major cracks are expected. Tensile tests of a #8 reinforcing bar embedded in concrete with a simulated crack opening were conducted with and without debonding in the region of the simulated crack opening. Debonding was achieved by decoupling the reinforcing bar from the concrete using polyolefin shrink tubes tightly fitting over the bar after heating. Experimental results showed that debonding of 8 in (203 mm) on each side of the simulated crack increased the peak displacement by about 38 percent compared to the case without debonding.

Computational analyses were conducted using a detailed finite element model that has been validated against experimental results. The model showed that using the debonding method resulted in an improvement of more than 30 percent in the peak vertical load-carrying capacity under a column removal scenario, without a significant degradation in the seismic resistance of the beam-column assembly. The proposed approach thus enhances the resistance of reinforced concrete frames to disproportionate collapse. Additional work is required to evaluate the efficiency of this debonding technique in more complex loading conditions and other configurations and detailing.

REFERENCES

1. American Concrete Institute (ACI), *Building code requirements for structural concrete and commentary*, ACI 318-02 and ACI 318R-02, Farmington Hills, MI, 2002.

2. Bao, Y., Lew, H.S., and Kunnath, S., "Modeling of reinforced concrete assemblies under a column removal scenario," *Journal of Structural Engineering*, 2012 (In press, available online at http://dx.doi.org/10.1061/(ASCE) ST.1943-541X.0000773).

3. Hallquist, J., *LS-DYNA Keyword User's Manual*, Livermore Software Technology Corporation, Livermore, CA, Version 971, 2007.

4. Lew, H. S., Bao, Y., Pujol S. and Sozen, M. A., "Experimental Study of RC assemblies under a Column Removal Scenario," *ACI Structural Journal*, (Accepted for publication), April 2013.

5. Su, Y., Tian, Y., and Song, X., "Progressive Collapse Resistance of Axially-restrained Frame Beams," *ACI Structural Journal*, V. 106, No. 5, Sep.-Oct. 2009, pp. 600-607.

6. Yi, W., He, Q., Xiao, Y., and Kunnath, S. K., "Experimental Study on Progressive Collapse-resistant Behavior of Reinforced Concrete Frame Structures," *ACI Structural Journal*, V. 105,

No. 4, Jul.-Aug. 2008, pp. 433-439.

7. Yu, J., and Tan, K. H., "Experimental and Numerical Investigation on Progressive Collapse Resistance of Reinforced Concrete Beam Column Sub-assemblages," Engineering Structures, In press (DOI:10.1016/j.engstruct.2011.08.040).

LIST OF FIGURES

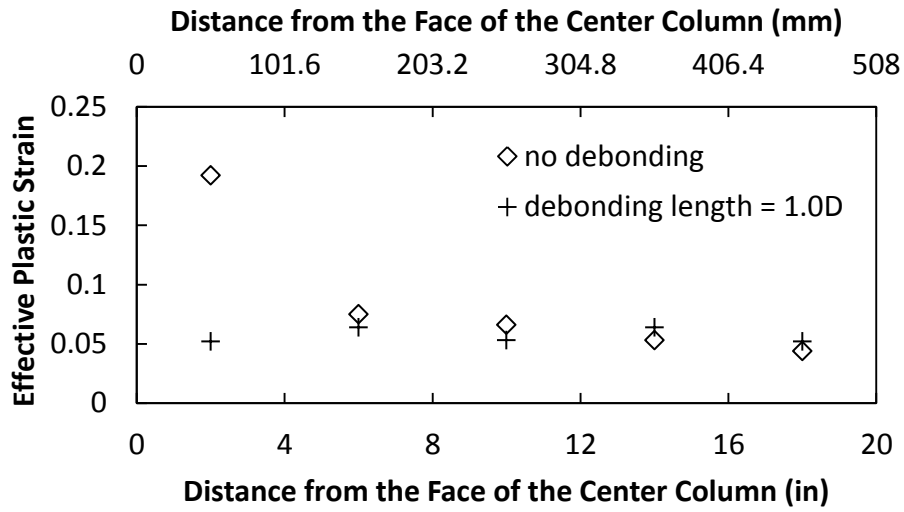Fig. 1 – Observed reinforcing bar fracture at beam-column assembly test.

Fig. 2 – Effective plastic strain distribution along bottom reinforcing bar in tension at a center column vertical displacement of 41 in (1041 mm).
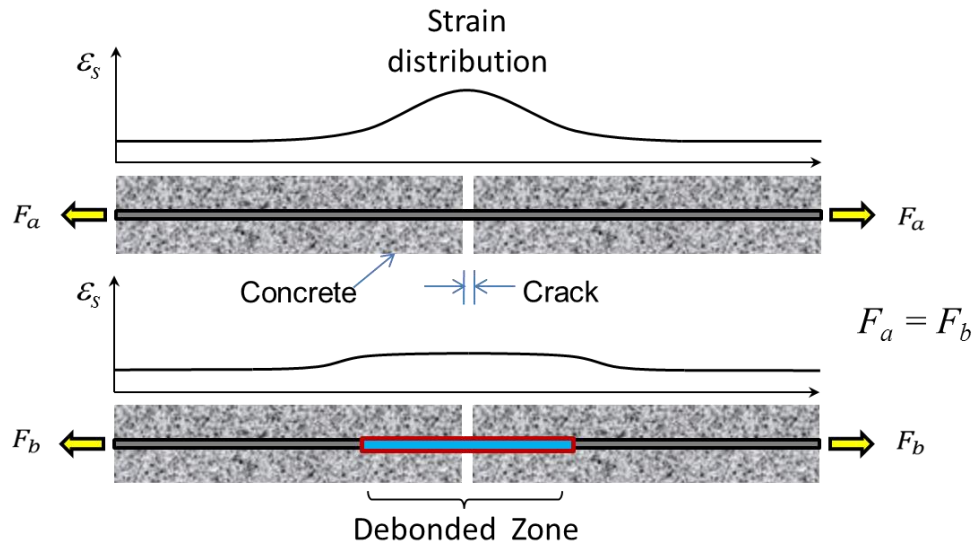
Fig. 3 – Debonding concept.

Fig. 4 – Test setup and specimen design. (1 inch = 25.4 mm).

Fig. 5 – Debonding technique using polyolefin shrink tube before and after heat application.

Fig. 6 – (a) No concrete damage on the free surface of the specimens with debonding; (b) cone-shaped concrete breakout on the free surface of the specimen without debonding

Fig. 7 – (a) Test results versus analysis results; (b) Finite element model and contour of concrete damage and reinforcing bar axial forces for Specimen C at peak load.

Fig. 8 – Applied vertical load versus vertical displacement of center column based on analysis of detailed finite element model with various values of debonding length.

Fig. 9 – Behavior under seismic loading: (a) Pushover; (b) Cyclic loading.

Fig. 1 – Observed reinforcing bar fracture at beam-column assembly test.

Fig. 2 – Effective plastic strain distribution along bottom reinforcing bar in tension at a center column vertical displacement of 41 in (1041 mm).
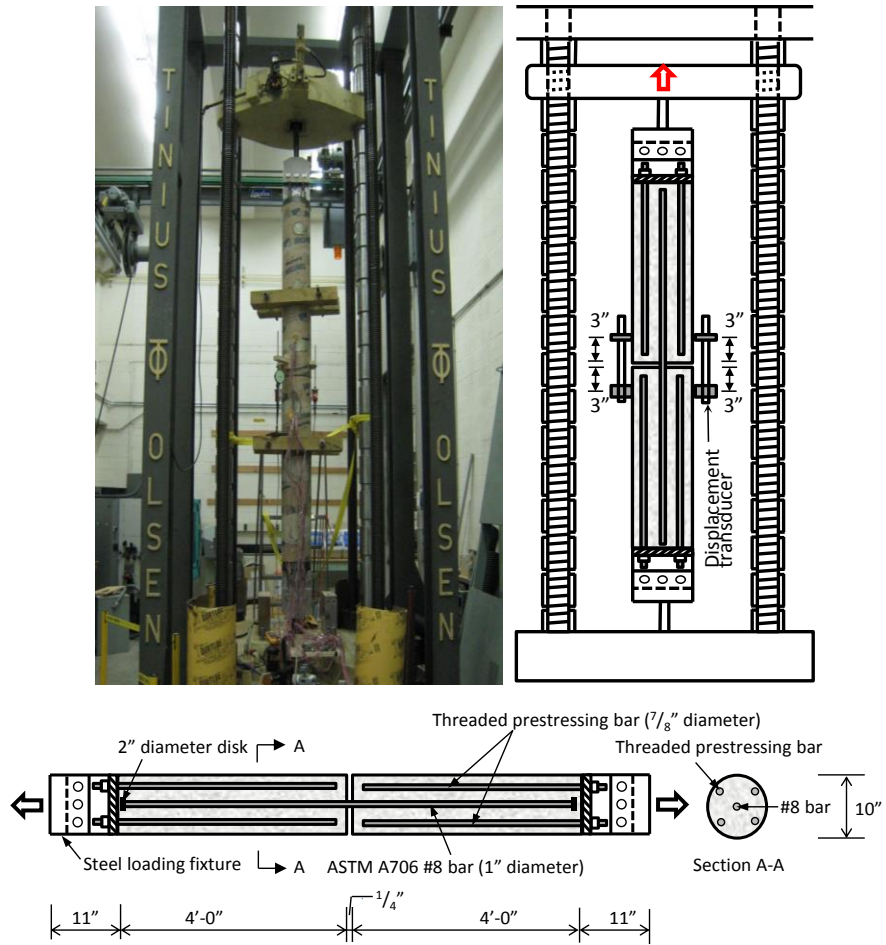
Fig. 3 – Debonding concept.

Fig. 4 – Test setup and specimen design. (1 inch = 25.4 mm)

Fig. 5 – Debonding technique using polyolefin shrink tube before and after heat application.

Fig. 6 – (a) No concrete damage on the free surface of the specimens with debonding; (b) cone-shaped concrete breakout on the free surface of the specimen without debonding.
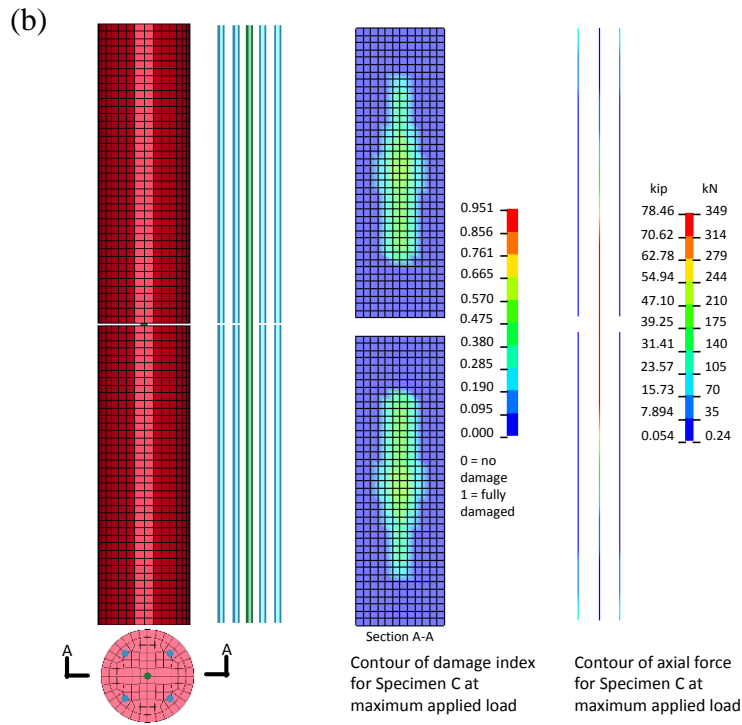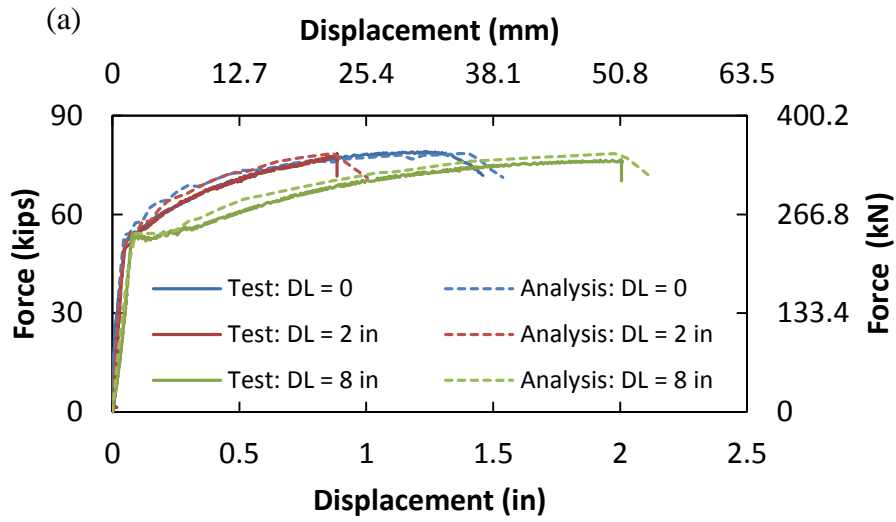
(a)

Displacement (mm)

(b)

Section A-A

Contour of damage index for Specimen C at maximum applied load

Contour of axial force for Specimen C at maximum applied load

Fig. 7 – (a) Test results versus analysis results; (b) Finite element model and contour of concrete damage and reinforcing bar axial forces for Specimen C at peak load.
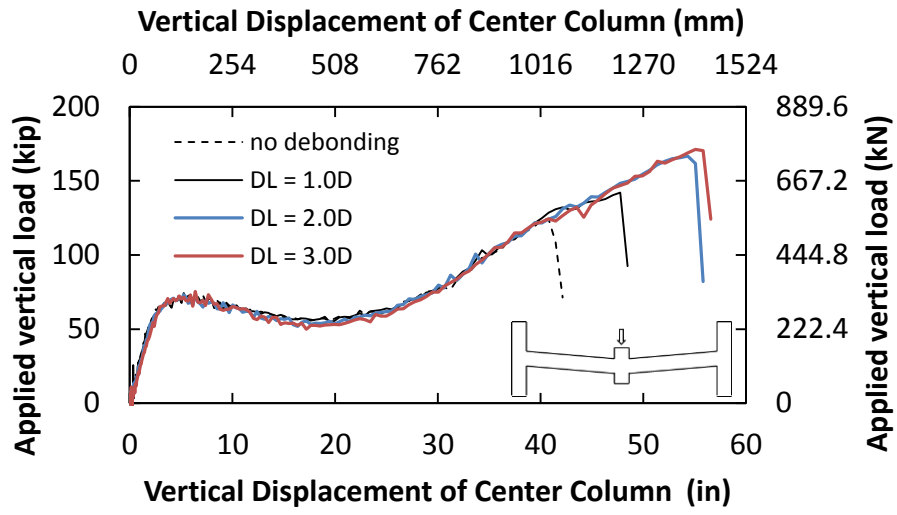
Fig. 8 – Applied vertical load versus vertical displacement of center column based on analysis of detailed finite element model with various values of debonding length.
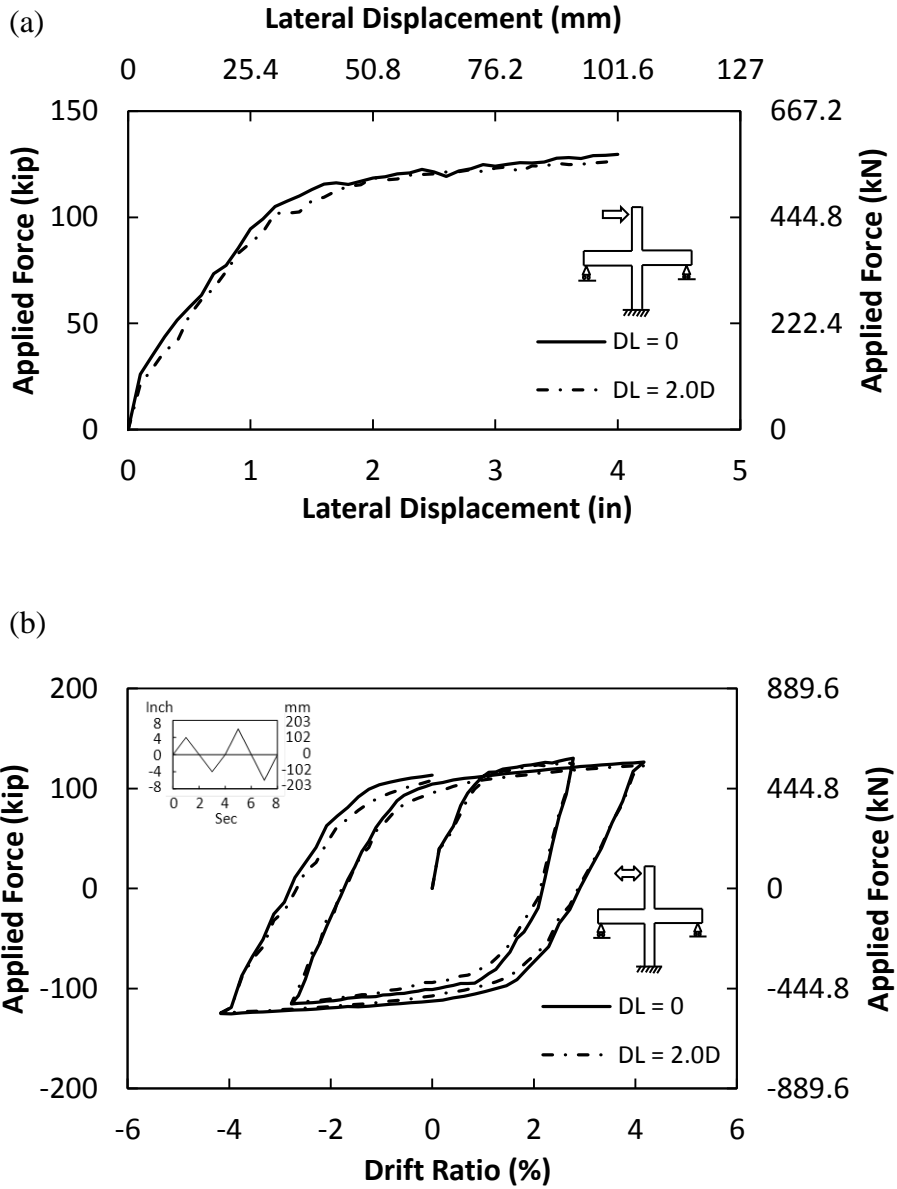
Fig. 9 – Behavior under seismic loading: (a) Pushover; (b) Cyclic loading.